

## ON THE ORIGIN OF RADIO EMISSION FROM MAGNETARS

ANDRZEJ SZARY<sup>1</sup>, GEORGE I. MELIKIDZE<sup>1,2</sup>, JANUSZ GIL<sup>1</sup>*Draft version August 1, 2022*

## ABSTRACT

Magnetars are the most magnetized objects in the known universe. Powered by the magnetic energy, and not by the rotational energy as in the case of radio pulsars, have long been regarded as a completely different class of neutron stars. The discovery of pulsed radio emission from a few magnetars weakened the idea of a clean separation between magnetars and normal pulsars. We use the Partially Screened Gap (PSG) model to explain radio emission of magnetars. The PSG model requires that the temperature of the polar cap is equal to the so-called critical value, i.e. the temperature at which the thermal ions outflowing from the stellar surface screen the acceleration gap. We show that a magnetar has to fulfill the ‘temperature’, ‘power’ and ‘visibility’ conditions in order to emit radio waves. Firstly, in order to form PSG the residual temperature of the surface has to be lower than the critical value. Secondly, since the radio emission is powered by the rotational energy it has to be high enough to enable heating of the polar cap by backstreaming particles to the critical temperature. Finally, the structure of magnetic field has to be altered by magnetospheric currents in order to widen a radio beam and increase the probability of detection. Our approach allows to predict whether a magnetar can emit radio waves using only its rotational period, period derivative and surface temperature in the quiescent mode.

*Keywords:* stars: neutron — stars: magnetars — pulsars: general

## 1. INTRODUCTION

From the historical reasons magnetars were divided into two distinct classes, AXPs and SGRs (Anomalous X-ray Pulsars and Soft Gamma Repeaters), based on the way they were discovered. However, nowadays it is widely accepted that those objects are highly magnetized neutron stars, which can explain the properties of both AXPs and SGRs (Thompson & Duncan 1995; Mereghetti 2008). Unlike other neutron stars for which emission is powered by rotational energy, accretion, or heat of a star, the high-energy emission of magnetars is powered by the energy of their strong magnetic field. Assuming dipolar configuration of magnetic field and that the observed spin-down is caused by the emission of a rotating dipole in vacuum<sup>3</sup>, we can estimate the field strength at the polar cap as  $B_d \approx 6.4 \times 10^{19} \sqrt{P\dot{P}}$  G, where  $P$  is rotational period in seconds, and  $\dot{P}$  is period derivative. Using this formula we can estimate the magnetic field of magnetars at the stellar surface of the order  $\sim 10^{14} - 10^{15}$  G. However, this argument by itself cannot be treated as the final evidence that the magnetic field is so strong due to, for example, unknown contribution of other processes to the observed torque (e.g., magnetar wind, Harding et al. (1999)). Nevertheless, analysis of spectral and energy properties of AXPs/SGRs further confirmed strong magnetic fields of magnetars (see review paper by Mereghetti 2013).

In the last few years it has been realized that the sep-

aration between magnetars and pulsars is not as sharp as previously considered. It is believed that the radio emission of pulsars is powered by the rotational energy of the star (also called spin-down luminosity)  $L_{SD} = \dot{E} = 4\pi^2 I \dot{P} P^{-3} \simeq 3.95 \times 10^{31} I_{45} \left( \dot{P}/10^{-15} \right) (P/s)^{-3} \text{ erg s}^{-1}$ , where  $I = 10^{45} I_{45} \text{ g cm}^2$  is the star’s moment of inertia. As we will show in the accompanying paper (Szary et al. 2014a) radio emission of pulsars mainly depends on details of charged particles acceleration in close vicinity of the pulsar’s polar cap (an altitude  $\lesssim 10^4$  cm). X-ray observations of old radio pulsars show that the hot spot surface, and thereby the actual polar cap, is much smaller than would result from the purely dipolar geometry. Using the flux conservation law we can estimate the magnetic field strength in the acceleration region being of the order of  $\sim 10^{14}$  G. The open question is why most magnetars do not emit radio waves since plasma responsible for radio emission is accelerated in similar conditions as in radio pulsars. Based on the observed sample of radio magnetars, Melikidze et al. (2011); Rea et al. (2012) suggested that magnetars can be radio active when the quiescent X-ray luminosity is smaller than the spin-down luminosity. However, as showed by the latest spectral fits by Viganò et al. (2013) it is not the case for XTE J1810-197 (see Table 1).

In this paper, we study whether the inner acceleration region of magnetars can be described by the same model as in normal radio pulsars, namely the Partially Screened Gap (PSG) model. Since most magnetars are radio quiet, we are focusing on finding conditions which should be met to form PSG, and hence to produce plasma responsible for radio emission.

aszary@astro.ia.uz.zgora.pl

<sup>1</sup> Kepler Institute of Astronomy, University of Zielona Góra, Lubuska 2, 65-265 Zielona Góra, Poland

<sup>2</sup> Abastumani Astrophysical Observatory, Ilia State University, 3-5 Cholakashvili Ave., Tbilisi, 0160, Georgia

<sup>3</sup> Although the assumptions are unrealistic, more realistic models (e.g., Spitkovsky 2006) give values within factor of two from the simplified formula.

**Table 1**

Observed properties of magnetars. The individual columns are as follows: (1) Number of the magnetar, (2) Magnetar name, (3) Rotational period, (4) Period derivative, (5) Magnetic field strength at the polar cap, (6) Spin-down luminosity, (7) Radius of the polar cap, (8) Critical temperature (see Equation 1), (9) Observed temperature, (10) Power required to heat up the polar cap to the critical temperature (see Equation 2), (11) Observed X-ray luminosity, (12) Reference. Magnetars are sorted by name (2).

No.	Name	$P$ (s)	$\dot{P}$ ( $10^{-11} \text{ s s}^{-1}$ )	$B_d$ ( $10^{14} \text{ G}$ )	$\log L_{\text{SD}}$ ( $\text{erg s}^{-1}$ )	$R_{\text{pc}}$ (m)	$T_{\text{crit}}$ ( $10^6 \text{ K}$ )	$T_{\text{bb}}$ ( $10^6 \text{ K}$ )	$\log L_{\text{heat}}$ ( $\text{erg s}^{-1}$ )	$\log L_{\text{bb}}$ ( $\text{erg s}^{-1}$ )	Ref.
1	1E 1048.1-5937	6.46	1.25 – 5.00	5.75 – 11.50	33.26 – 33.87	59	7.43 – 12.49	7.43	31.28 – 32.18	33.80 – 34.50	1, 2
2	1E 1547.0-5408	2.07	2.60 – 9.78	4.70 – 9.11	35.06 – 35.64	104	6.38 – 10.49	6.03	31.51 – 32.37	34.30 – 34.70	3, 4, 2
3	1E 1841-045	11.79	4.09	14.06	32.99	44	14.52	5.57	32.18	35.20 – 35.50	5, 2
4	1E 2259+586	6.98	0.05	1.18	31.75	57	2.26	4.64	29.17	35.00 – 35.40	5, 2
5	1RXS J170849.0-400910	11.01	1.95	9.36	32.76	45	10.71	5.22	31.68	34.80 – 35.10	5, 2
6	3XMM J185246.6+003317	11.56	0.01	0.81	30.55	44	1.71	–	28.48	30.78	6
7	4U 0142+61	8.69	0.20	2.68	32.09	51	4.19	4.76	30.15	35.40 – 35.80	5, 7
8	CXOU J010043.1-721134	8.02	1.88	7.86	33.16	53	9.39	4.06	31.59	35.20 – 35.50	8, 2
9	CXOU J164710.2-455216	10.61	0.04	1.32	31.12	46	2.46	3.83	29.14	33.10 – 33.60	9, 2
10	CXOU J171405.7-381031	3.83	5.88 – 10.50	9.60 – 12.83	34.62 – 34.87	77	10.91 – 13.56	6.27	32.17 – 32.55	34.90 – 35.20	10, 2
11	PSR J1622-4950	4.33	0.94 – 1.94	4.09 – 5.86	33.66 – 33.98	72	5.75 – 7.54	5.80	31.01 – 31.48	32.64	11, 12
12	SGR 0418+5729	9.08	0.004	0.12	29.32	50	0.41	3.71	26.11	30.70 – 31.10	13
13	SGR 0501+4516	5.76	0.59	3.74	33.09	62	5.38	6.61	30.77	33.20 – 34.00	14, 2
14	SGR 0526-66	8.05	3.80	11.20	33.46	53	12.24	5.57	32.05	35.40 – 35.80	15, 2
15	SGR 1627-41	2.59	1.90	4.49	34.63	93	6.17	5.22	31.35	34.40 – 34.80	16, 17, 2
16	SGR 1806-20	7.55	8.27 – 79.00	15.99 – 49.42	33.88 – 34.86	55	15.99 – 37.28	8.01	32.54 – 34.01	35.10 – 35.50	18, 2
17	SGR 1833-0832	7.57	0.35	3.29	32.50	55	4.89	–	30.48	33.00 – 35.00	19, 20
18	SGR 1900+14	5.20	6.13 – 20.00	11.42 – 20.64	34.24 – 34.75	66	12.43 – 19.37	4.53	32.26 – 33.04	35.00 – 35.40	21, 2
19	SGR J1745-2900	3.76	0.61 – 1.39	3.07 – 4.62	33.66 – 34.01	77	4.64 – 6.30	–	30.69 – 31.23	32.04	22, 23
20	Swift J1822.3-1606	8.44	0.002 – 0.01	0.27 – 0.54	30.15 – 30.74	52	0.75 – 1.25	6.27	27.18 – 28.07	32.90 – 33.20	24, 2
21	Swift J1834.9-0846	2.48	0.80	2.84	34.31	95	4.38	–	30.77	30.92	25, 26
22	XTE J1810-197	5.54	0.43 – 1.04	3.12 – 4.87	33.00 – 33.38	64	4.70 – 6.55	3.02	30.55 – 31.12	34.00 – 34.40	27, 28, 2

**References.** (1) Dib et al. 2009, (2) Viganò et al. 2013, (3) Dib et al. 2012, (4) Bernardini et al. 2011, (5) Dib & Kaspi 2014, (6) Rea et al. 2014, (7) Rea et al. 2007, (8) McGarry et al. 2005, (9) An et al. 2013, (10) Sato et al. 2010, (11) Levin et al. 2010, (12) Anderson et al. 2012, (13) Rea et al. 2013, (14) Camero et al. 2014, (15) Tiengo et al. 2009, (16) Esposito et al. 2009, (17) Esposito et al. 2009, (18) Woods et al. 2007, (19) Esposito et al. 2011, (20) Göğüş et al. 2010, (21) Mereghetti et al. 2006, (22) Kaspi et al. 2014, (23) Mori et al. 2013, (24) Scholz et al. 2014, (25) Kargaltsev et al. 2012, (26) Younes et al. 2012, (27) Camilo et al. 2007, (28) Bernardini et al. 2011

## 2. PARTIALLY SCREENED GAP

The acceleration gap above the polar cap can form if a local charge density is lower than the co-rotational charge density (Goldreich & Julian 1969). The charge depletion in this region depends on the binding energy of the positive  $^{56}\text{Fe}$  ions in the crust. The binding energy, and thus emission of iron ions from the condensed stellar surface was calculated by Medin & Lai (2007). The critical temperature, i.e. the temperature at which charge density of ions is equal to the co-rotational charge density, can be described as:

$$T_{\text{crit}} \approx 2.0 \times 10^6 B_{14}^{0.75}, \quad (1)$$

where  $B_{14} = B_s / (10^{14} \text{ G})$  is a surface magnetic field at the polar cap. Spectral fits to the X-ray data of old radio pulsars show that the temperature of polar caps is about a few millions Kelvin. Furthermore, the X-ray observations allow to indirectly determine the surface magnetic field of radio pulsars using the magnetic flux conservation law  $B_s = B_d A_{\text{pc}} / A_{\text{bb}}$ , here  $A_{\text{pc}} \approx 6.2 \times 10^4 P^{-1} \text{ m}^2$  is the conventional polar cap area (assuming purely dipolar configuration of magnetic field) and  $A_{\text{bb}}$  is the observed polar cap area. Although still the subject of controversy as the X-ray observations are burdened with large uncertainties, the observed temperature and the magnetic field strength at the polar cap of radio pulsars agree with the theoretical predictions of the critical temperature (see, e.g., Szary 2013, and references therein). In order to form PSG and explain both radio and thermal X-ray emissions of normal pulsars, the surface magnetic field has to be dominated by very strong crust anchored magnetic anomalies (Gil et al. 2002; Szary 2013), thus  $B_s \sim 10^{14} \text{ G} \gg B_d$ .

The basic features of the PSG model (Gil et al. 2003) are as follows. The supply rate of positive charges from the stellar surface is not enough to compensate the outflow of charges through the light cylinder. As a consequence, it leads to the development of a potential drop above the polar cap. The backstreaming electrons accelerated in the gap heat the polar cap. Depending on the mode, the polar cap is either overheated by electrons leading to its breakdown (the PSG-off mode), or the temperature is kept close, but still below, the critical temperature (the PSG-on mode, Szary et al. (2014a)). In the PSG-on mode the surface temperature  $T_s$  is thermostatically regulated leading to a continuous outflow of iron ions which leads to a partial screening of the acceleration potential drop. The gap breakdown in the PSG-on mode is due to production of dense electron-positron plasma ( $\rho_p \gg \rho_{\text{GJ}}$ ) which is responsible for generation of radio emission at higher altitudes. Regardless of the mode in which PSG operates, the observed temperature of a few millions Kelvin requires the magnetic field of the order of  $10^{14} \text{ G}$  (see Equation 1). Since the dipolar component of the magnetic field at the polar cap of normal radio pulsars is of the order of  $10^{12} \text{ G}$ , formation of PSG requires much stronger, and thus highly non-dipolar magnetic field at the polar cap. Note, that the non-dipolar configuration of surface magnetic field was proposed from the very beginning of pulsars astronomy, e.g. the Vacuum Gap model (Ruderman & Sutherland 1975) requires highly non-dipolar radius of curvature,  $\mathcal{R} \approx 10^6 \text{ cm}$ , in order to enable absorption of  $\gamma$ -photons in a gap region and electron-positron pair production. In the case of magnetars, on the other hand, the dipolar component of the magnetic field at the surface already

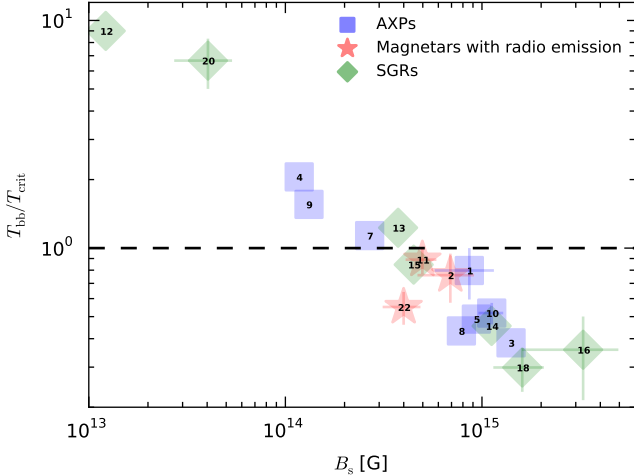


**Figure 1.** Ratio of the observed surface/spot temperature to the predicted critical temperature of the polar cap. The horizontal axis corresponds to the value of the inferred magnetic field at the polar cap. The red stars correspond to the magnetars with detected radio emission.

fulfills the PSG model requirement of strong magnetic field  $\sim 10^{14}$  G. Furthermore, in one of the modes of PSG (namely the PSG-on mode) inverse Compton scattering is responsible for  $\gamma$ -photon emission in a gap region. Even assuming dipolar curvature of magnetic field lines, due to the high energy of such  $\gamma$ -photons they are easily converted to electron-positron pairs. Thus, unlike normal pulsars, for magnetars it is not required to have a non-dipolar configuration of surface magnetic field to form PSG. Geppert et al. (2013); Geppert & Viganò (2014) showed that the Hall drift is the physical process that can be responsible for production of small-scale strong surface magnetic field anomalies on time-scales of  $10^4$  yr. The time-scale suggest that magnetars, as young neutron stars, should be characterized by a dipolar surface magnetic field. The surface magnetic field of normal radio pulsars, on the other hand, should be dominated by magnetic spots produced by means of non-linear interaction between poloidal and toroidal components of the subsurface magnetic field.

### 3. RESULTS

#### 3.1. Temperature

It is widely believed that magnetars are very young neutron stars. As the approach to calculate the characteristic age,  $\tau_c$ , assumes that the observed period is much longer than the rotational period at birth,  $\tau_c$  can be poor approximation for their true age. Indeed, even relatively low mean velocity of magnetars (Tendulkar et al. 2013) does not explain their very small Galactic scale height. Further evidence comes from estimates of ages of their host supernovas, thus, for example, the age of the CTB 109 (14 kyr) is much shorter than the characteristic age of the magnetar 1E 2259+586 ( $\tau_c = 230$  kyr). As young neutron stars, magnetars tend to have high residual temperature. We mentioned in Section 2 that PSG can form if surface temperature is lower than the critical value. Thus, we can define the first condition that must be met in order to allow formation of PSG, and hence generation of radio emission. Namely, the residual temperature has to be lower than the critical value  $T_{bb} < T_{crit}$ . In Figure

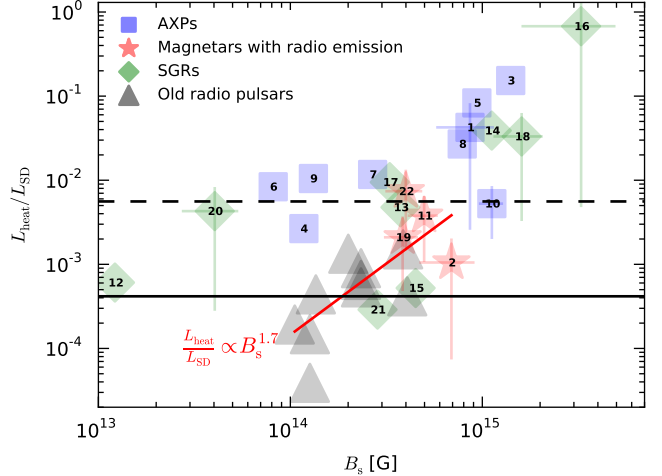


**Figure 2.** Ratio of power required to heat up the polar cap to the critical temperature to the spin-down luminosity. The gray triangles show the observed thermal X-ray efficiency of radio pulsars. The red stars correspond to magnetars with detected radio emission. The solid and dashed black horizontal lines correspond to the median and maximum values of the observed X-ray efficiency of radio pulsars, respectively. The red solid line correspond to the linear fit for sources with radio emission (both magnetars and old radio pulsars).

1 we present ratio of the observed residual temperature to the predicted critical temperature of the polar cap. Confirming the hypothesis, all the magnetars with detected radio emission have residual temperature below the critical value. Note that due to the fact that the residual temperature of SGR J1745-2900 is not known it was not included in the figure. However, taking into account the upper limit for its X-ray luminosity in the quiescence mode,  $L_{bb} = 1.1 \times 10^{32}$  erg s $^{-1}$ , the whole surface temperature of this magnetar is well below the critical value  $T_{bb} = 6 \times 10^5$  K  $\ll 4.6 \times 10^6$  K ( $T_{bb}$  was calculated assuming  $R_{bb} = 10$  km). Taking into account the temperature condition, we find that as long as the surface temperature will not decrease below the critical value the following magnetars cannot generate radio emission: 1E 2259+586, 4U 0142+61, CXOU J164710.2-455216, SGR 0418+5729, SGR 0501+4516, Swift J1822.3-1606.

#### 3.2. Power

The high-energy radiation of magnetars (X-rays and  $\gamma$ -rays) during the active state is powered by the magnetic energy. Since the radio emission of magnetars appears only after the X-ray outburst it was believed that the magnetic energy is also a source of energy of the radio emission. However, based on the observed sample of radio magnetars, Melikidze et al. (2011); Rea et al. (2012) suggested that the radio emission from magnetars might be powered by the rotational energy. In normal radio pulsar particles are accelerated in the inner acceleration region at the expense of rotational energy giving the raise to plasma responsible for both radio emission and pulsar wind. If the plasma responsible for radio emission of magnetars is produced and accelerated in PSG (as in the case of radio pulsars) it should also be powered by the rotational energy.

The strength of magnetic field at the polar cap of magnetars is of the order of  $\sim 10^{14} - 10^{15}$  G. Knowing the critical temperature (see Equation 1) and size of the po-

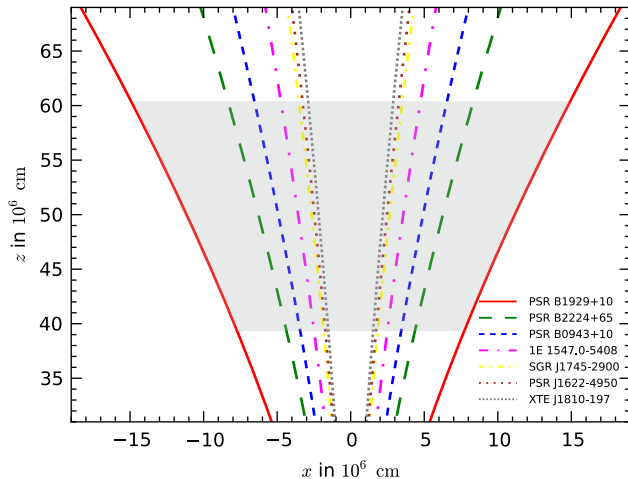


**Figure 3.** Comparison of open field lines regions of radio magnetars and a sample of radio pulsars. The lines correspond to the last open magnetic field line.

lar cap,  $A_{pc}$ , we can estimate power required to heat up the polar cap to the critical temperature:

$$L_{\text{heat}} = \sigma A_{pc} T_{\text{crit}}^4, \quad (2)$$

where  $\sigma$  is the Stefan-Boltzmann constant. In Figure 2 we plot the ratio of power required to heat up the polar cap to the critical temperature to the spin-down luminosity. For magnetars with detected radio emission less than about one percent of rotational energy is enough to heat up the polar cap. In the figure we present also efficiency of X-ray emission of the polar cap for radio pulsars,  $L_{pc}/L_{SD}$ . Note that an estimation of an actual surface magnetic field of a pulsar is possible only for old sources for which radiation of the whole surface and the non-thermal magnetospheric X-ray emission do not dominate the X-ray spectrum. Similarly to radio magnetars, all radio pulsars are characterized by the polar cap radiation with luminosity considerably smaller than the spin-down luminosity  $L_{pc}/L_{SD} < 1\%$ . We argue that magnetar can generate radio waves only if its spin-down luminosity is high-enough, i.e.  $L_{\text{heat}}/L_{SD} \lesssim 1\%$ . Moreover, the power-law fit for all sources active in radio results in the following relationship:

$$L_{pc, \text{heat}}/L_{SD} \propto B_s^{1.7}. \quad (3)$$

It clearly shows that with increasing strength of the surface magnetic field at the polar cap, neutron stars active in radio (both pulsars and magnetars) use greater part of its rotational kinetic energy to heat up the polar cap to the critical temperature, and thus to form partially screened gap. Taking into account the power condition we find that the radio emission of the following magnetars will be possible only after a significant decay of the magnetic field: 1E 1841-045, 1RXS J170849.0-400910, CXOU J010043.1-721134, SGR 0526-66. Furthermore, taking into account the observational uncertainties the radio emission is unlikely to appear from the following sources: 1E 1048.1-5937, SGR 1806-20, SGR 1900+14.

### 3.3. Visibility

In Sections 3.1 and 3.2 we have shown the conditions which can be used to determine whether a magnetar can

be active in radio. They are based on an assumption that plasma responsible for radio emission of magnetars is produced in the same manner as in radio pulsars (i.e. pair creation and acceleration in PSG). However, we know from observations that in some aspects properties of magnetars radio emission are different than the properties of pulsars radio emission. Firstly, in magnetars radio emission is not continues and it appears only after the X-ray outburst. Secondly, the radio pulse profiles and fluxes varies on a time scales from minutes to days. Finally, the average radio flux decays with decaying X-ray flux of the outburst. The bundle of open field lines of magnetars is much smaller than the one of normal pulsars. Beloborodov (2009) suggested that it may result in narrow radio beam, and thus is small probability of its passing through our line of sight. As a consequence, when a magnetar is in quiescence the radio pulsations are hardly detectable. The situation changes during the outburst when the magnetosphere is twisted. The magnetospheric currents alter the magnetic field in the region where radio emission is generated, thereby broadening the radio beam. As the magnetosphere untwists, the size of the radio beam returns to its original small size. Using the simple model (see, e.g., Lorimer & Kramer (2004)) we can write that the opening angle of radio beam is

$$\rho \approx 0.4^\circ R_{\text{em}}^{0.5} P^{-0.5}, \quad (4)$$

here  $R_{\text{em}}$  is the emission height in kilometers. Although, the consensus regarding the radio emission process itself has not been established yet, the emission height is one of its aspect which is the least problematic. The PSG model, similarly as the Vacuum Gap model (Ruderman & Sutherland 1975), is the non-stationary model of the inner acceleration region. In such a model, the sparking-like gap discharges leads to the creation of pair plasma clouds. The plasma clouds consist of particles with a large spectrum of energies and move along the magnetic field lines. Particles from successive clouds overlap with each other due to different energies, i.e. high energy particles from a latter cloud overlap with lower energy particles from the earlier cloud. As shown by Asseo & Melikidze (1998) this will result in an efficient two-stream instability which triggers electrostatic Langmuir waves. The electrostatic oscillations are unstable which results in formation of plasma solitons with a characteristic length along magnetic field lines of about 30 cm, thus making them capable of emitting coherent curvature radiation at radio wavelengths Melikidze et al. (2000). In the described model, the emission height is defined as a place where particles from two consecutive clouds overlap leading to a two-stream plasma instability. The time after which particles with different Lorentz factors will overcome each other can be estimated as  $t_r \sim h/(2\Delta v)$ , where  $h$  is the gap height, and  $\Delta v \sim c/(2\gamma_p^2)$  is the velocity difference, here  $\gamma_p$  is the average Lorentz factor of secondary plasma. Note the factor of 2 difference in the formula with the one presented in Melikidze et al. (2000). The difference is due to the fact that the Vacuum Gap model assumes that the plasma clouds are of the same size as the gap height, while in the PSG model the plasma clouds are considerably smaller than  $h$ . Furthermore, the Vacuum Gap model predicts the dependence of the gap height on pulsar period, dipolar component of magnetic

field and curvature radius in the gap region. However, our latest studies (Szary et al. 2014b) have shown that the radio luminosity does not depend on rotational parameters  $P$  and  $\dot{P}$ . The result suggest that plasma responsible for radio emission is created and accelerated in similar conditions regardless of the dipolar component of the magnetic field. Indeed, in Szary et al. (2014a) we show that for wide ranges of magnetic field strength at the surface and curvature radius the gap height does not vary essentially and is of the order of  $h \sim 50R$ . Finally, using typical value for the average Lorentz factor of generated plasma,  $\gamma_p \approx 10^2$ , we can estimate the emission height as  $R_{em} \approx t_{rc} \approx h\gamma_p^2 \sim 50R$ , where  $R$  is the neutron star radius. Note that the emission height may vary from pulsar (or magnetar) to another, but as we have shown above, there is no theoretical justification that in magnetars the emission height should be higher than in normal radio pulsars. In Figure 3 we show the comparison of last open magnetic field lines for a sample of radio pulsars and magnetars with detected radio emission. It clearly shows, that due to their longer periods magnetars are characterized by smaller radio beam. During the outburst curvature of open magnetic field lines of magnetars can significantly change resulting in much larger opening angle of radio emission. Furthermore, in the quiescent state of a magnetar, the curvature of magnetic fields lines in the radio emission region is smaller than the one of radio pulsars which may be of importance for radio emission process. It is also worth noting that during the outburst the flux of X-ray background photons increases, thereby facilitating inverse Compton scattering in the acceleration region, and thus the gap breakdown.

#### 4. CONCLUSIONS

There are ongoing large theoretical and observational efforts to find when and which magnetar will emit radio waves. It was argued that in principle any magnetar undergoing an outburst could be radio active. Moreover, it was believed that whatever the mechanism of radio emission is, it should be different from that of rotation-powered radio pulsars. In this paper we show that both above statements are not true. Furthermore, we show that not only the observed sample of radio magnetars can be explained within the framework of the PSG model, but we can use its predictions to establish whether a newly discovered magnetar will generate pulsed radio emission or not. Note that predictions regarding radio activity or inactivity of magnetars were performed assuming that the magnetic field at the polar cap does not differ significantly from purely dipolar solution. However, especially for the low field magnetars, it may not be the case. As recently shown by Tiengo et al. (2014), the energy of proton cyclotron absorption line in the X-ray spectrum of SGR 0418+5729 implies a magnetic field ranging from  $2 \times 10^{14}$  G to more than  $10^{15}$  G. The existence of small-scale, strong, multipolar components in an active magnetar is yet another feature that makes boundaries between magnetars and radio pulsars fade.

This work is supported by National Science Centre Poland under grants 2011/03/N/ST9/00669 and DEC-2012/05/B/ST9/03924. The data used in the paper are

taken from the McGill magnetars catalog (Olausen & Kaspi 2014)<sup>4</sup> and the catalog of isolated neutron stars with clearly observed thermal emission in quiescence by (Viganò et al. 2013)<sup>5</sup>.

#### REFERENCES

- An H., Kaspi V. M., Archibald R., Cumming A., 2013, *ApJ*, 763, 82
- Anderson G. E., Gaensler B. M., Slane P. O., Rea N., Kaplan D. L., Posselt B., Levin L., Johnston S., Murray S. S., Brogan C. L., Bailes M., Bates S., Benjamin R. A., Bhat N. D. R., 2012, *ApJ*, 751, 53
- Asseo E., Melikidze G. I., 1998, *MNRAS*, 301, 59
- Beloborodov A. M., 2009, *ApJ*, 703, 1044
- Bernardini F., Israel G. L., Stella L., Turolla R., Esposito P., Rea N., Zane S., Tiengo A., Campana S., Götz D., Mereghetti S., Romano P., 2011, *A&A*, 529, A19
- Bernardini F., Perna R., Gotthelf E. V., Israel G. L., Rea N., Stella L., 2011, *MNRAS*, 418, 638
- Camero A., Papitto A., Rea N., Viganò D., Pons J. A., Tiengo A., Mereghetti S., Turolla R., Esposito P., Zane S., Israel G. L., Götz D., 2014, *MNRAS*, 438, 3291
- Camilo F., Cognard I., Ransom S. M., Halpern J. P., Reynolds J., Zimmerman N., Gotthelf E. V., Helfand D. J., Demorest P., Theureau G., Backer D. C., 2007, *ApJ*, 663, 497
- Dib R., Kaspi V. M., 2014, *ApJ*, 784, 37
- Dib R., Kaspi V. M., Gavril F. P., 2009, *ApJ*, 702, 614
- Dib R., Kaspi V. M., Scholz P., Gavril F. P., 2012, *ApJ*, 748, 3
- Esposito P., Burgay M., Possenti A., Turolla R., Zane S., de Luca A., Tiengo A., Israel G. L., Mattana F., Mereghetti S., Bailes M., Romano P., Götz D., Rea N., 2009, *MNRAS*, 399, L44
- Esposito P., Israel G. L., Turolla R., Mattana F., Tiengo A., Possenti A., Zane S., Rea N., Burgay M., Götz D., Mereghetti S., 2011, *MNRAS*, 416, 205
- Esposito P., Tiengo A., Mereghetti S., Israel G. L., De Luca A., Götz D., Rea N., Turolla R., Zane S., 2009, *ApJ*, 690, L105
- Gil J., Melikidze G. I., Geppert U., 2003, *A&A*, 407, 315
- Gil J. A., Melikidze G. I., Mitra D., 2002, *A&A*, 388, 235
- Goldreich P., Julian W. H., 1969, *ApJ*, 157, 869
- Gögüş E., Cusumano G., Levan A. J., Kouveliotou C., Sakamoto T., Barthelmy S. D., Campana S., Kaneko Y., Stappers B. W., 2010, *ApJ*, 718, 331
- Harding A. K., Contopoulos I., Kazanas D., 1999, *ApJ*, 525, L125
- Kargaltsev O., Kouveliotou C., Pavlov G. G., Gögüş E., Lin L., Wachter S., Griffith R. L., Kaneko Y., Younes G., 2012, *ApJ*, 748, 26
- Geppert, U., Gil, J., & Melikidze, G. 2013, *MNRAS*, 435, 3262
- Geppert, U., & Viganò, D. 2014, *MNRAS*, 444, 3198
- Kaspi V. M., Archibald R. F., Bhalariao V., Dufour F., Gotthelf E. V., An H., Bachetti M., Beloborodov A. M., Boggs S. E., Christensen F. E. e. a., 2014, *ApJ*, 786, 84
- Levin L., Bailes M., Bates S., Bhat N. D. R., Burgay M., Burke-Spolaor S., D'Amico N., Johnston S., Keith M., Kramer M., Milia S., Possenti A., Rea N., Stappers B., van Straten W., 2010, *ApJ*, 721, L33
- Lorimer D. R., Kramer M., 2004, *Handbook of Pulsar Astronomy*
- McGarry M. B., Gaensler B. M., Ransom S. M., Kaspi V. M., Veljkovic S., 2005, *ApJ*, 627, L137
- Medin Z., Lai D., 2007, *MNRAS*, 382, 1833
- Melikidze, G. I., Gil, J. A., & Pataraya, A. D. 2000, *ApJ*, 544, 1081
- Melikidze, G., Gil, J., & Szary, A. 2011, *American Institute of Physics Conference Series*, 1379, 144
- Mereghetti S., 2008, *A&A Rev.*, 15, 225
- Mereghetti S., 2013, *Brazilian Journal of Physics*, 43, 356
- Mereghetti S., Esposito P., Tiengo A., Zane S., Turolla R., Stella L., Israel G. L., Götz D., Feroci M., 2006, *ApJ*, 653, 1423
- Mori K., Gotthelf E. V., Zhang S., An H., Baganoff F. K., Barrière N. M., Beloborodov A. M., Boggs S. E., Christensen F. E. e. a., 2013, *ApJ*, 770, L23
- Olausen S. A., Kaspi V. M., 2014, *ApJS*, 212, 6

<sup>4</sup> [www.physics.mcgill.ca/~pulsar/magnetar/main.html](http://www.physics.mcgill.ca/~pulsar/magnetar/main.html)

<sup>5</sup> [www.neutronstarcooling.info](http://www.neutronstarcooling.info)

- Rea N., Israel G. L., Pons J. A., Turolla R., Viganò D., Zane S., Esposito P., 2013, *ApJ*, 770, 65
- Rea N., Nichelli E., Israel G. L., Perna R., Oosterbroek T., Parmar A. N., Turolla R., Campana S., Stella L., Zane S., Angelini L., 2007, *MNRAS*, 381, 293
- Rea N., Pons J. A., Torres D. F., Turolla R., 2012, *ApJ*, 748, L12
- Rea N., Viganò D., Israel G. L., Pons J. A., Torres D. F., 2014, *ApJ*, 781, L17
- Ruderman, M. A., & Sutherland, P. G. 1975, *ApJ*, 196, 51
- Sato T., Bamba A., Nakamura R., Ishida M., 2010, *PASJ*, 62, L33
- Scholz P., Kaspi V. M., Cumming A., 2014, *ApJ*, 786, 62
- Spitkovsky A., 2006, *ApJ*, 648, L51
- Szary A., 2013, arXiv:1304.4203, PhD Thesis
- Szary A., Melikidze G., Gil J., 2014a, *MNRAS*, accepted, *'Two modes of Partially Screened Gap'*, arXiv:1412.3093
- Szary, A., Zhang, B., Melikidze, G. I., Gil, J., & Xu, R.-X. 2014b, *ApJ*, 784, 59
- Tendulkar S. P., Cameron P. B., Kulkarni S. R., 2013, *ApJ*, 772, 31
- Thompson C., Duncan R. C., 1995, *MNRAS*, 275, 255
- Tiengo A., Esposito P., Mereghetti S., Israel G. L., Stella L., Turolla R., Zane S., Rea N., Götz D., Feroci M., 2009, *MNRAS*, 399, L74
- Tiengo A., Esposito P., Mereghetti S., Turolla R., Nobili L., Gastaldello F., Götz D., Israel G. L., Rea N., Stella L., Zane S., Bignami G. F., 2014, *Astronomische Nachrichten*, 335, 274
- Viganò D., Rea N., Pons J. A., Perna R., Aguilera D. N., Miralles J. A., 2013, *MNRAS*, 434, 123
- Woods P. M., Kouveliotou C., Finger M. H., Göğüş E., Wilson C. A., Patel S. K., Hurley K., Swank J. H., 2007, *ApJ*, 654, 470
- Younes G., Kouveliotou C., Kargaltsev O., Pavlov G. G., Göğüş E., Wachter S., 2012, *ApJ*, 757, 39